ISBN: 978-3-95450-214-1 ISSN: 2673-5490 doi:10.18429/JACoW-IPAC2021-TUPAB236

PROGRESS ON THE ELECTRON GUN DESIGN FOR A McMILLAN ELECTRON LENS IN THE FERMILAB INTEGRABLE OPTICS TEST ACCELERATOR (IOTA)

B. Cathey*, G. Stancari, Fermi National Accelerator Laboratory, Batavia IL, U.S.A.

Abstract

This paper covers the progress made so far in designing the first McMillan electron lens for the Fermilab IOTA ring. The novel design allows for an increase in tune spread without limiting the dynamic aperture due to its integrability. Shown are simulations for an electron gun design to generate the specific required current density distribution for the nonlinear integrable system in IOTA.

INTRODUCTION

As circular accelerators achieve higher beam intensities, beam instabilities increasingly limit design capabilities. Beam instabilities can come from interactions of the beam with the surrounding environment through wakefields and impedance, or from space charge due to the beam itself. Landau damping is one way to mitigate instabilities. Landau damping is the use of a spread of betatron tunes, called a tune spread, to lower a beam's sensitivity to instabilities. To generate a tune spread nonlinear forces are required, such as octupole magnets creating tune spread dependent on the particle's amplitude. However, octupoles and other nonlinear elements can have a significant drawback in that they reduce the beam's dynamic aperture. Fortunately, there are nonlinear dynamical systems that are integrable, and therefore can be implemented in accelerators without loss of dynamic aperture [1–6].

The Integrable Optics Test Accelerator (IOTA) at Fermilab is dedicated in part to the experimental study of novel, integrable, nonlinear focusing lattices [7]. In particular, one straight section is designed to include an electron lens, which will be used for research on nonlinear dynamics, electron cooling, and space-charge compensation [7–9]. Because of their flexibility, electron lenses can be designed to have different effects on the circulating beam [10–14]. In this paper, we focus on the design of an electron gun for the IOTA electron lens as a nonlinear focusing element for the implementation of the McMillan integrable system [15].

BACKGROUND

The McMillan system can be broken into two sections: a linear transport and a nonlinear kick [2, 3]. The linear transport requires a 0.25 phase advance in both vertical and horizontal phase spaces, and a round beam at the kick. The two dimensional McMillan kick is defined as,

$$f(r) = \frac{kr}{\frac{r^2}{a^2} + 1}, \tag{1}$$

with k as the kick strength and a as an effective width. This kick can generate a wide tune spread while the system maintains integrability [16]. Its shape and radial nature make an electron lens ideal for implementation. There are two regimes of strength for the McMillan lens based on the beta function of the circulating beam. The weak regime occurs when $\beta k < 2$ and has a maximum tune spread of

$$(\Delta\nu)_{\max} = \frac{1}{4} - \frac{1}{2\pi}\arccos\left(\frac{\beta k}{2}\right). \tag{2}$$

The strong regime is when $\beta k > 2$ and can create a tune spread that reaches the integer resonance. The McMillan lens will need to access both regimes for IOTA.

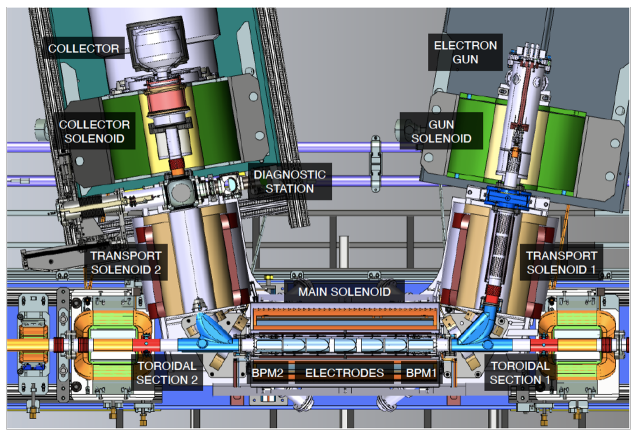

Figure 1: Drawing of the electron lens in IOTA.

IOTA was designed with the capability of giving the above requirements for phase advance and beam shape. Phase advances can be designated with 10^{-3} accuracy, and beta functions within 1% [9]. The electron lens, currently under development for IOTA, is shown schematically in Fig. 1. The lens beam will be delivered into and out of IOTA using a system of solenoids and toroids. The interaction region occurs throughout the main solenoid, which is 0.7 m long. The magnets will maintain the McMillan beam shape from the gun to the collector, providing slight focusing. The electron gun, inside the gun solenoid, will be responsible for generating the beam that produces the McMillan kick.

The McMillan kick can be generated from a current density of the form,

$$j(r) = \frac{j_0 a^4}{\left(r^2 + a^2\right)^2}, \tag{3}$$

where j_0 is the on axis beam current density and a corresponds to the same parameter in Eq. (1). This gives a kick

* bcathey@fnal.gov

ISBN: 978-3-95450-214-1 ISSN: 2673-5490 doi:10.18429/JACoW-IPAC2021-TUPAB236

strength of,

$$k = \frac{2\pi j_0 L(1 \pm \beta_e \beta_z)}{(B\rho)_z \beta_e \beta_z c^2} \left(\frac{1}{4\pi\epsilon_0} \right). \quad (4)$$

Here, β_z and $(B\rho)_z$ are the speed and rigidity of the circulating beam, β_e is the speed of the electron lens beam, and L is the length of the lens. The sign is determined by whether the electron lens is co-propagating (-) or counter-propagating (+). For this implementation, the beams will be co-propagating, slightly limiting the kick strength. Figure 2 shows the shape of the McMillan lens current density for several values of a.

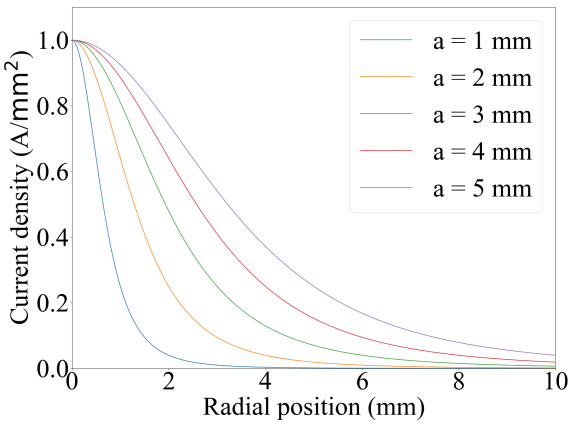

Figure 2: The current density required for the McMillan electron lens for different values of effective width a.

The current density in Eq. (3) corresponds to a total current of

$$I = \pi a^2 j_0. \quad (5)$$

The design beta function in IOTA at the lens location is 4 m, which puts the weak/strong lens transition at $k = 0.5$ m^{-1}. For a 150 MeV circulating electron beam in IOTA, this corresponds to $j_0 = 10$ A/cm^2 in the overlap region for a typical 5 keV electron-lens.

THE McMILLAN ELECTRON GUN

The McMillan gun will use electrodes with a shaped cathode to generate the necessary beam. The design attempts to use a cathode radius of 10 mm to guarantee coverage of the full transverse area and allow for kicked beam studies [16]. This creates an immediate challenge as a lower a is harder to achieve the larger the cathode. To keep the desired beam shape after emission, the gun is immersed inside a solenoid with a strong magnetic field. Initial designs were studied using WARP simulations [17]. A similar application where the current-density profile is critical is the RHIC Gaussian electron gun [18, 19]. A general design was ascertained by studying the electric field close to the cathode surface, because the field is the main factor determining current density in the space-charge-limited regime. This showed that a traditional hemispherical cathode could not produce the needed current distribution, but a Gaussian cathode was able to create the needed field. Figure 3 shows the Gaussian cathode, and Fig. 4 compares the resulting electric field along the cathode surface to an ideal McMillan current density. The good agreement gives a starting point, however, WARP is only able to emit off of a flat or hemispherical surface. Work is ongoing to have Gaussian emission implemented in WARP.

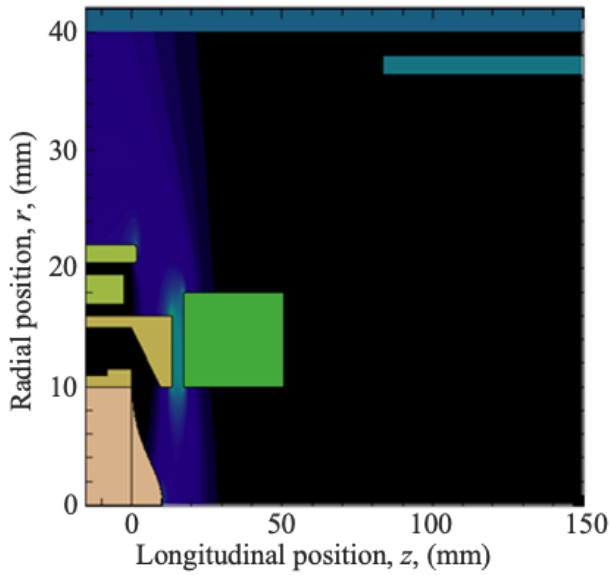

Figure 3: Gaussian cathode simulation in WARP to calculate the electric field along the cathode surface.

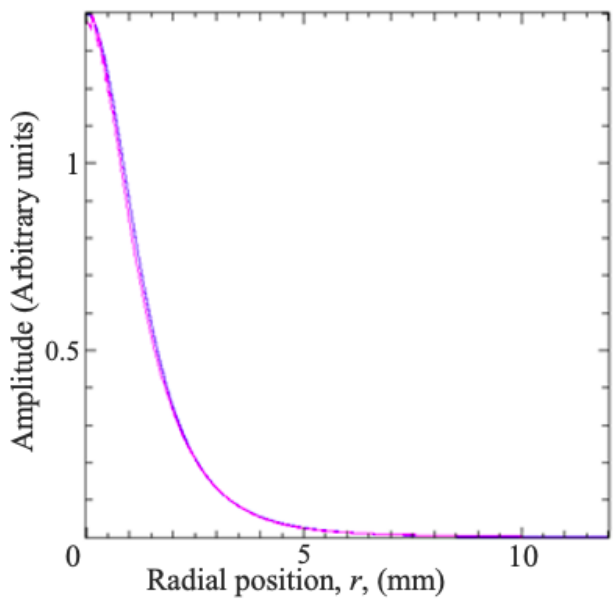

Figure 4: A comparison between an ideal McMillan current density (blue) and the electric field strength along the surface of a Gaussian cathode in WARP (magenta).

Gun design has continued using COMSOL, which allows for a Gaussian emission surface [20]. Starting with the

ISBN: 978-3-95450-214-1 ISSN: 2673-5490 doi:10.18429/JACoW-IPAC2021-TUPAB236

general design above from WARP, different parameters are being scanned through to optimize the gun. Of particular import are the Gaussian parameters (amplitude and sigma), the cathode base width, the control electrode position, and the anode position. The resultant beam is integrated over a volume downstream of the anode to get a projection along the radial axis to determine the current density of the simulation. The ideal McMillan current density can be linearized to the form of

$$\sqrt{\left(\frac{j_0}{j(r)}\right)^{\frac{1}{2}} - 1} = \frac{1}{a}r. \tag{6}$$

The inverse of the slope then gives a. Therefore for a simulated beam, the closest ideal McMillan shape can be determined by linearizing the resultant current density by Eq. (6), and finding the slope of the best fit. It should be noted that a recreation of the RHIC gun [18, 19] in COMSOL resulted in a matching current density shape, but the on axis and total current did not match. As such, the COMSOL results are normalized. The reason for the discrepancy is being investigated. Further benchmarking can be done with known simulations and measurements of existing electron guns.

A possibly viable current density was generated by the design in Fig. 5. The design was immersed in a 0.5 T magnetic field. Figure 6 shows the linearized current density from the design. The result matches the straight line very well, and the fitted slope gives an a of 4.1 mm. Figure 7 directly compares the normalized simulated current density with an ideal McMillan profile with a = 4.1 mm. As expected from the linear graph, the two are very similar.

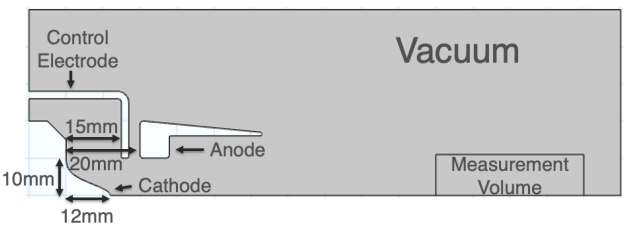

Figure 5: An electron gun design for generating a McMillan lens electron beam. The cathode, electrode, and anode are displayed in negative space. Aside from the notable parameters shown, the cathode surface has a Gaussian sigma of 3 mm.

CONCLUSIONS

These results show that the necessary lens current density for the McMillan system is physically achievable with a shaped cathode. Further simulations need to be done to optimize the design, paying particular attention to the electric field strength between the control electrode and anode where electrical breakdown may happen. Also underway is a study into the McMillan lens's operation tolerances. While early results show the system to be robust, an in-depth study

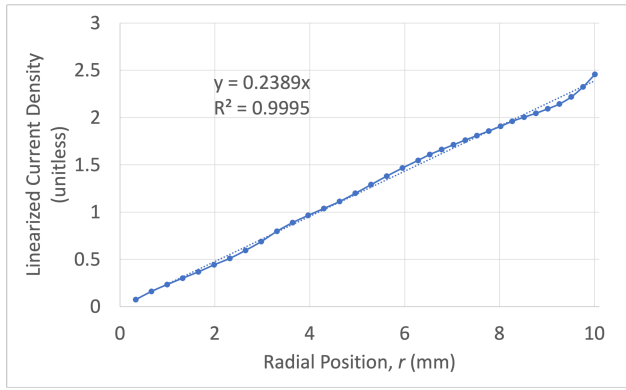

Figure 6: The linearized current density from the gun design in Fig. 5. The resulting value of a is 4.1 mm.

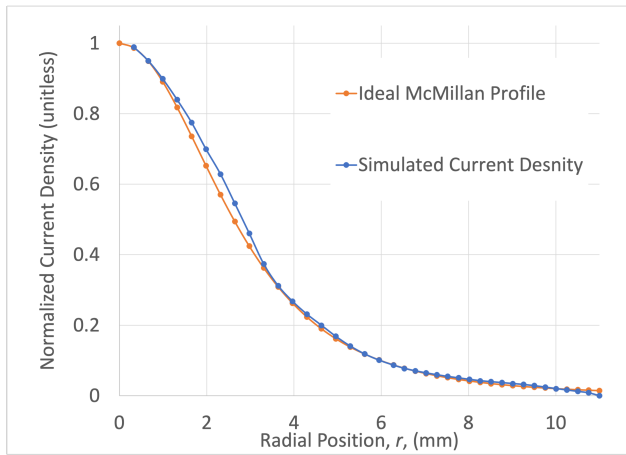

Figure 7: A comparison between the normalized current density from the gun design in Fig. 5 and an ideal McMillan profile with an a value of 4.1 mm.

is necessary to determine how close the lens needs to be to the ideal charge density for an experimental demonstration of the concept.

Once a design is finalized, the electron gun can be manufactured. Its charge density will be tested at the Fermilab electron lens test stand before insertion into the IOTA electron lens.

ACKNOWLEDGMENTS

This manuscript has been authored by Fermi Research Alliance, LLC under Contract No. DE-AC02-07CH11359 with the U.S. Department of Energy, Office of Science, Office of High Energy Physics. Report no. FERMILAB-CONF-21-238-AD.

REFERENCES

[1] A. G. Ruggiero, "Integrability of the two-dimensional beam-beam interaction in a special case," *Part. Accel.*, vol. 12, pp. 45–47, 1982.

[2] V. V. Danilov and E. A. Perevedentsev, "On invariants and integrability in nonlinear accelerator optics," CERN, Geneva, Switzerland, Tech. Rep. SL-NOTE-94-74-AP, 1994.

ISBN: 978-3-95450-214-1 ISSN: 2673-5490 doi:10.18429/JACoW-IPAC2021-TUPAB236

[3] V. V. Danilov and E. A. Perevedentsev, "Two examples of integrable systems with round colliding beams," in *Proc. IEEE Particle Accelerator Conference (PAC'07)*, Vancouver, Canada, May 1997, pp. 1759–1761, doi:10.1109/pac.1997.750998

[4] V. V. Danilov and V. D. Shiltsev, "On possibility of footprint compression with one lens in nonlinear accelerator lattice," Fermilab, Batavia, IL, USA, Tech. Rep. FERMILAB-FN-671, 1998.

[5] V. Danilov and V. Shiltsev, "On the possibility of footprint compression with one lens in nonlinear accelerator lattice," *J. Instrum.*, vol. 16, no. 3, p. P03050, 2021, doi:10.1088/1748-0221/16/03/P03050

[6] V. Danilov and S. Nagaitsev, "Nonlinear accelerator lattices with one and two analytic invariants," *Phys. Rev. ST Accel. Beams*, vol. 13, no. 8, p. 084 002, Aug. 2010, doi:10.1103/PhysRevSTAB.13.084002

[7] S. Antipov *et al.*, "IOTA (Integrable Optics Test Accelerator): Facility and experimental beam physics program," *J. Instrum.*, vol. 12, no. 03, T03002, Mar. 2017, doi:10.1088/1748-0221/12/03/t03002

[8] G. Stancari, "Applications of electron lenses: Scraping of high-power beams, beam-beam compensation, and nonlinear optics," *AIP Conf. Proc.*, vol. 1777, p. 100 007, Jul. 2016, doi:10.1063/1.4965688

[9] G. Stancari *et al.*, "Beam physics research with the IOTA electron lens," *J. Instrum.*, vol. 16, no. 05, P05002, May 2021, doi:10.1088/1748-0221/16/05/p05002

[10] V. Shiltsev, Y. Alexahin, K. Bishofberger, V. Kamerdzhiev, G. Kuznetsov, and X.-L. Zhang, "Experimental demonstration of colliding-beam-lifetime improvement by electron lenses," *Phys. Rev. Lett.*, vol. 99, p. 244 801, 24 Dec. 2007, doi:10.1103/PhysRevLett.99.244801

[11] G. Stancari *et al.*, "Collimation with hollow electron beams," *Phys. Rev. Lett.*, vol. 107, p. 084 802, Aug. 2011, doi:10.1103/PhysRevLett.107.084802

[12] W. Fischer *et al.*, "Operational head-on beam-beam compensation with electron lenses in the Relativistic Heavy Ion Collider," *Phys. Rev. Lett.*, vol. 115, p. 264 801, 26 Dec. 2015, doi:10.1103/PhysRevLett.115.264801

[13] V. D. Shiltsev, *Electron Lenses for Super-Colliders*, New York, NY, USA: Springer, 2016.

[14] S. Redaelli *et al.*, "Hollow electron lenses for beam collimation at the High-Luminosity Large Hadron Collider (HL-LHC)," *J. Inst.*, vol. 16, no. 3, p. P03042, Mar. 2021, doi:10.1088/1748-0221/16/03/P03042

[15] E. M. McMillan, "A problem in the stability of periodic systems," *Topics in Modern Physics: A Tribute to Edward U. Condon*, pp. 219–244, 1971.

[16] B. Cathey, G. Stancari, A. Valishev, and T. Zolkin, "Calculations of detuning with amplitude for the McMillan electron lens in the Fermilab Integrable Optics Test Accelerator (IOTA)," *J. Instrum.*, vol. 16, no. 3, p. P03041, Mar. 2021, doi:10.1088/1748-0221/16/03/P03041

[17] Warp, http://warp.lbl.gov.

[18] A. Pikin, "Simulations of Gaussian electron guns for RHIC electron lens," BNL, Upton, NY, USA, Tech. Rep. BNL-104383-2014-IR, 2014.

[19] W. Fischer *et al.*, "Electron lenses in RHIC: Status and prospects," *J. Instrum.*, vol. 16, no. 3, p. P03040, Mar. 2021, doi:10.1088/1748-0221/16/03/p03040

[20] COMSOL Multiphysics, https://www.comsol.com.